JOC The Journal of Organic Chemistry

Article

pubs.acs.org/joc

Triphenylamine–Benzimidazole Derivatives: Synthesis, Excited-State Characterization, and DFT Studies

João Pina and J. Sérgio Seixas de Melo*

Department of Chemistry, University of Coimbra, P3004-535 Coimbra, Portugal

Rosa M. F. Batista, Susana P. G. Costa, and M. Manuela M. Raposo*

Center of Chemistry, University of Minho, Campus de Gualtar, 4710-057 Braga, Portugal

Supporting Information

ABSTRACT: The synthesis and comprehensive characterization of the excited states of four novel triphenylamine–benzimidazole derivatives has been undertaken in solution (ethanol and methylcyclohexane) at room temperature. This includes the determination of the absorption, fluorescence, and triplet–triplet absorption spectra, together with quantum yields of fluorescence, internal conversion, intersystem crossing, and singlet oxygen. From the overall data the radiative and radiationless rate constants could be obtained, and it is shown that the compounds are highly emissive with the radiative decay dominating, with more than 70% of the quanta loss through this deactivation channel. The basic structure of the triphenylamine–benzimidazole derivatives (**1a**) was modified at position 5 of the heterocyclic moiety with electron-donating (OH (**1b**), OCH_3 (**1c**)) or electron-withdrawing groups (CN, (**1d**)). It was found that the photophysical properties remain basically unchanged with the different substitutions, although a marked Stokes shift was observed with **1d**. The presence and nature of a charge-transfer transition is discussed with the help of theoretical (DFT and TDFT) data. All compounds displayed exceptionally high thermal stability (between 399 and 454 °C) as seen by thermogravimetric analysis.

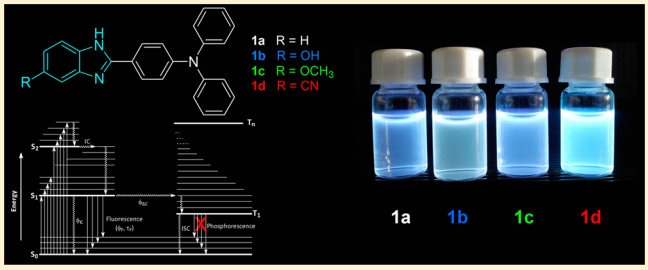

INTRODUCTION

Research on organic luminescent materials has been intensely pursued because of their importance in technological applications related to signaling, fluorescent biosensory/chemosensory materials, molecular switches, and organic light-emitting diodes (OLEDs).[1−5] Organic fluorophores such as triphenylamine and (benz)imidazole derivatives have attracted a particular attention owing to their high emission efficiency as well as their excellent thermal stability in guest–host systems, being widely used respectively as hole- and electron-transporters and emitting layers for OLEDs[6−12] as well as building blocks for the synthesis of efficient optical chemosensors due to their receptor/signaling ability to anions, cations or molecules.[13,14]

Crucial factors for successful OLEDs are a facile and balanced charge transport as well as a high conversion efficiency of excitons into light.[7] Generally, with the incorporation of electron-donor and -acceptor moieties in a single emitter it is possible to control the HOMO–LUMO energy level and to simultaneously balance the electron–hole recombination.[15−17] To improve the charge-transfer capability, a molecular structure that localizes the HOMOs and LUMOs at their respective hole- and electron-transporting moieties is desirable.[18,19] Furthermore, the emitting materials should possess amorphous morphology to decrease the crystallinity, which is preferable to improve the device performance. In a recent study electroluminescent devices fabricated using a triphenylamine-substituted benzimidazole derivative as the emitting layer, showed a high external quantum efficiency (EQE), of 4.67%, along with a high color purity of the blue emission.[20] This device performance was attributed to the bulky 3D structure of the investigated triphenylamine-benzimidazole derivative that limits the molecular packing density, therefore suppressing exciton quenching and in that way increasing the EQE.

In the field of molecular recognition, benzimidazole derivatives have also been extensively used for sensing of cations, anions, and neutral molecules due to the emissive properties of this heterocycle.[21−23] Other heterocyclic systems bearing functionalized (benz)imidazole derivatives exhibiting high thermal stability have also been recently investigated.[24,25] As a result, this moiety has been used not only as a binding unit for cations and anions, as the imidazole derivatives do, but also as a fluorogenic antenna.[13]

In another field of research, triphenylamine and its derivatives have displayed promising properties in the development of photovoltaic devices as donor moieties due in part to

Received: September 3, 2013
Published: October 11, 2013

   dx.doi.org/10.1021/jo401803u | J. Org. Chem. 2013, 78, 11389–11395

Scheme 1. Synthesis of Benzimidazoles 1a–d

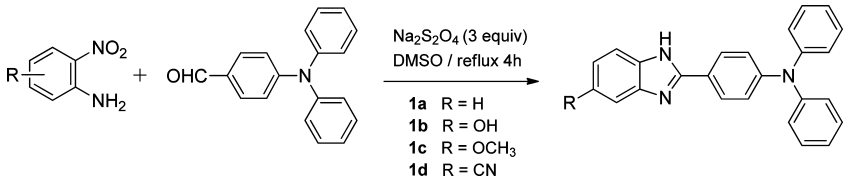

their chemical stability together with stabilized photoexcited state by charge delocalization in the aryl substituents. A recent study showed that the introduction of benzimidazole derivatives in the phenyl ring of the triphenylamine core increases the molar extinction coefficients together with absorption maxima (due to the increased π-conjugation), and a overall improved photovoltaic performance was obtained when compared to the unsubstituted counterpart.[26]

In the present work, we focus on the synthesis and photophysical characterization of new triphenylamine–benzimidazoles bearing groups of different electronic nature (electron donor or acceptor) at position 5 of the benzimidazole ring, in order to gain detailed understanding of the relationship between structure and its deactivation pathways.

RESULTS AND DISCUSSION

The structures of the investigated compounds are depicted in Scheme 1, consisting of triphenylamine–benzimidazole derivatives substituted at position 5 of the benzimidazole heterocycle with different electron-donating (OH, OMe) or electron-withdrawing groups (CN).

Synthesis and Characterization. Triphenylamine–benzimidazoles **1a–d** bearing groups of different electronic nature (electron donor or acceptor) at position 5 of the benzimidazole ring were synthesized in good to excellent yields (87–95%) by a one-step reaction through the $Na_2S_2O_4$ reduction[24,27] of several commercially available *o*-nitroanilines in the presence of triphenylamine aldehyde in DMSO at 120 °C (Table 1, Scheme 1).

Table 1. Yields, IR, and T_d Data for Compounds 1a–d

compd	R	yield (%)	IR $\bar{\nu}^a$ (cm^{-1})	$T_d{}^b$ (°C)
1a	H	89	3401 (NH)	399
1b	OH	87	3320 (NH); 3646 (OH)	406
1c	OMe	91	3354 (NH)	413
1d	CN	95	3410 (NH); 2229 (CN)	454

[a]Recorded in nujol. [b]Decomposition temperature (T_d) measured at a heating rate of 20 °C min^{-1} under nitrogen atmosphere, obtained by TGA.

Thermal Stability of Triphenylamine–Benzimidazoles 1a–d. Thermal stability of compounds **1a–d** was studied by thermogravimetric analysis (TGA), measured at a heating rate of 20 °C min^{-1} under a nitrogen atmosphere. The results obtained revealed the exceptional high thermal stability for all compounds, which could be heated up to T_d = 399–454 °C. Moreover, the introduction of electron donor (OMe, OH) or electron acceptor (CN) groups at the benzimidazole moiety led to highly thermal stable materials (T_d = 406–454 °C) compared to the unsubstituted derivative **1a** (T_d = 399 °C).

Spectroscopic and Photophysical Properties. The electronic spectra and photophysical properties of compounds **1a–1d** were investigated in ethanol at T = 293K. It is worth noting that the photophysical properties here obtained are not restricted to the fluorescence properties, but to all the deactivation processes, ϕ_F, ϕ_{IC}, ϕ_T, and also the singlet oxygen sensitization yield, ϕ_Δ, which allows a thorough analysis of the decay processes occurring with these compounds. For the sake of simplicity, the discussion will be mainly focused on properties of these new compounds, as seen by what we can consider the model compound, **1a**, and the effect of the different donor (**1b** and **1c**) and acceptor (**1d**) substituents at the benzimidazole chromophore.

Substituent groups have a marked effect in the spectroscopic (shift in both absorption and fluorescence spectra) and photophysical properties of many organic compounds. In general, electron-donating groups induce an increase in the molar absorption coefficient and enhance the fluorescence efficiency (ϕ_F), whereas electron-withdrawing groups reduce the fluorescence quantum yield.[28]

Figure 1 presents the absorption and fluorescence emission spectra of compounds **1a–d** in ethanol solution. From the

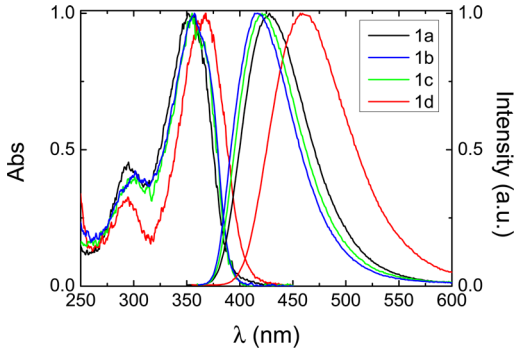

Figure 1. Room-temperature absorption and fluorescence emission (collected with λ_{exc}= 350 nm) spectra for the investigated triphenylamine–benzimidazoles in ethanol solution.

absorption and fluorescence emission spectra it can be seen that the electron-withdrawing CN group in compound **1d** originates the most pronounced shift both in the absorption and emission spectra; indeed, **1d** displays a 13 nm (absorption) and 32 nm (emission) red-shift when compared to **1a**. However, when substitution is now made with electron-donor groups (compounds **1b** and **1c**) a negligible red-shift in the absorption band is observed whereas in the emission spectra a relatively marked spectral blue-shift is seen, again when compared to **1a**; see Figure 1 and Table 2.

For the triphenylamine–benzimidazole derivatives the observed large Stokes shift values found (in the range 3973–5583 cm^{-1} in ethanol and 2151–3136 cm^{-1} in methylcyclohexane solution, see Table 2) points out to the occurrence of an ICT process[29–32] between the donor (triphenylamine) unit and the electron-acceptor benzimidazole moiety. Indeed, the values are distinctly higher in ethanol than in methylcyclohexane; see Table 2. This behavior is in agreement to what was previously

dx.doi.org/10.1021/jo401803u | J. Org. Chem. 2013, 78, 11389–11395

Table 2. Spectroscopic Data (Absorption, Fluorescence Emission, and Triplet Absorption Maxima, Extinction-Singlet and Triplet-Coefficients, ε_{SS} and ε_{TT}, Stokes Shift, Δ_{SS}, and the Optical Absorption Band Gap, E_g) for the Triphenylamine–benzimidazoles Derivatives in Ethanol and Methylcyclohexane (MCH) Solutions at 293 K (Underlined Values Are the Wavelength Maxima)

compd	λ_{max}^{Abs} (nm)	λ_{max}^{Abs} cal [f][a] (nm)	ε_{SS} (M^{-1} cm^{-1})	λ_{max}^{Fluo} (nm)	$\lambda_{max}^{T_1 \rightarrow T_n}$ (nm)	ε_{TT} (M^{-1} cm^{-1})	Δ_{SS} (cm^{-1})	E_g (eV)
1a	295, 353	308, 360	19370	428	640	18100	4964	3.21
(MCH)	(298, 352)	[0.1771, 0.9219]		(382, 400)			(2151)	
1b	300, 357	309, 363	19400	416	650	12900	3973	3.22
(MCH)	(288, 350)	[0.1739, 0.9626]		(402)			(3136)	
1c	300, 355	300, 352	25230	421	650	17900	4416	3.22
(MCH)	(299, 355)	[0.1744, 0.9933]		(384, 403)			(2530)	
1d	295, 366	303, 372	22470	460	650	10200	5583	3.06
(MCH)	(294, 366)	[0.1660, 0.9419]		(399, 418)			(2260)	

[a] f: theoretical oscillator strength.

reported for triphenylamine-substituted benzimidazole derivatives where the longer wavelength absorption band around 340 nm was attributed to the charge transfer (CT) $\pi-\pi^*$ transition from the electron-donating triphenylamine moiety to the electron-accepting benzimidazole moiety[16,20] and are further confirmed by theoretical calculations (see below).

Fluorescence lifetimes were obtained with picosecond and nanosecond time resolution and were seen to fit to single exponential decay law (see Figure 2 and Table 2), which excludes energy transfer and conformational relaxation processes.[33,34] The values of 2–4 ns are typically those usually found for systems with D–A moieties.[35,36] However, as mentioned, even in a picosecond time scale the compounds were found single exponential, which apparently mirrors the rigid nature of the molecular structure of the compounds.

The triplet states of the triphenylamine–benzimidazole derivatives were characterized from the singlet–triplet difference transient absorption spectra (Figure 3). In addition to ground-state depletion at shorter wavelengths the spectra present an intense and broad triplet absorption in the 400–700 nm region. Although the clear signal observed (which are quenched by oxygen and display triplet lifetimes in the μs range, see Table 3), the intersystem crossing quantum yields, ϕ_T, are low with the lowest value for **1d**.

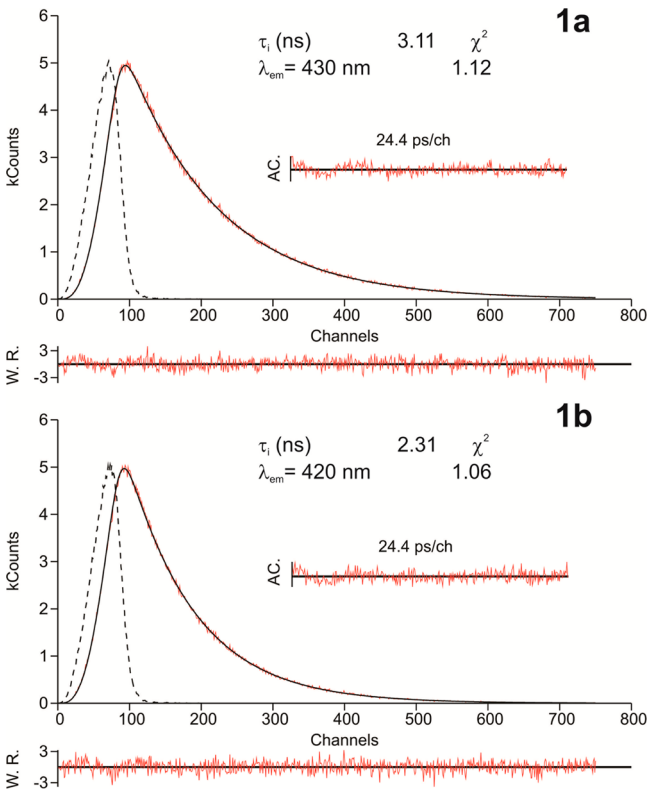

Figure 2. Room-temperature fluorescence decays for **1a** and **1b** in ethanol solution obtained with λ_{exc} = 373 nm and T = 293 K. For a better judgment of the quality of the fits, autocorrelation functions (AC), weighted residuals (WR), and χ^2 values are also present as insets. The dashed lines in the decays are the pulse instrumental response.

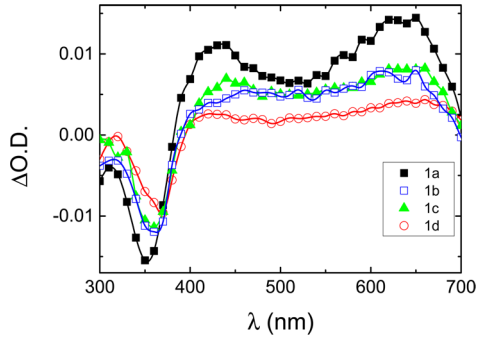

Figure 3. Room-temperature transient triplet–triplet absorption spectra for **1a–d** in ethanol solution at T = 293 K.

Singlet oxygen formation quantum yields (ϕ_Δ) were also obtained for the investigated compounds (Table 3) and were found to be close to the triplet intersystem crossing yields, thus giving essentially support for the latter values, but also showing that this is an inefficient route and that these compounds are likely to display photostability.

Table 3 presents the overall set of photophysical parameters including quantum yields, lifetimes, and rate constants obtained in ethanol solution at 293 K. For all the compounds an intense blue fluorescence with high ϕ_F values (0.70–0.78) is observed. Very interestingly, one can observe that the (high) ϕ_F values are higher than the value (0.50) previously reported for the *N,N,N′,N′*-tetraphenyl-5′-(1-phenyl-1*H*-benzimidazol-2-yl)-1,1′:3′,1″-terphenyl-4,4″-diamine derivative.[16] However, the obtained ϕ_F values are in good agreement to what was recently reported for mono- and ditriphenylamine-substituted 1,2-diphenylbenzimidazole derivatives (ϕ_F = 0.72 and 0.66, respectively).[20] Moreover, the constancy observed in the ϕ_F values shows that the substitution either with electron-donating

dx.doi.org/10.1021/jo401803u | J. Org. Chem. 2013, 78, 11389–11395

Table 3. Photophysical Properties Including Quantum Yields (Fluorescence, ϕ_F, Internal Conversion, ϕ_{IC}, Triplet formation, ϕ_T, and Sensitized Singlet Oxygen formation, ϕ_Δ) for 1a−d in Ethanol Solution and T = 293 K

compd	ϕ_F	τ_F (ns)	k_F (ns^{-1})	k_{NR} (ns^{-1})	k_{ISC} (ns^{-1})	ϕ_{IC}	k_{IC} (ns^{-1})	ϕ_T	ϕ_Δ	τ_T (μs)
1a	0.75	3.11	0.241	0.080	0.028	0.16	0.052	0.09	0.08	7.7
1b	0.71	2.31	0.307	0.126	0.043	0.19	0.082	0.10	0.05	3.3
1c	0.70	2.49	0.281	0.120	0.027	0.23	0.093	0.07	0.06	16
1d	0.78	3.97	0.196	0.055	0.010	0.18	0.045	0.04	0.05	87

or -withdrawing groups do not change significantly the photophysical properties of the compounds and is also in agreement to what was previously found for diphenyl-substituted benzimidazoles incorporating electron-donor or -acceptor groups (ϕ_F values in the 0.46−0.54 range).[37] A further split of the radiationless deactivation pathways (ϕ_T and ϕ_{IC}) can be made from the balance $\phi_{IC} = 1 - \phi_T - \phi_F$. The data show that the radiationless internal conversion channel, although with contributions of 26% to 23%, represents ca. 1/4 to the total *quanta* loss. This is further complemented with the determination of the rate constants for all the deactivation processes, where it can be seen that the radiative rate constant, k_F, is 1 order of magnitude higher than the intersystem crossing rate constant, k_{ISC}, and approximately 3 (**1b** and **1c**) to 5 (**1a** and **1d**) higher than the internal conversion rate constant, k_{IC}.

Summarizing at this stage, from the overall data for the triphenylamine-benzimidazoles derivatives **1a−d** the radiative channel is the main excited-state deactivation pathway, although the radiationless internal conversion decay route can be considered a competitive route for the deactivation of the excited state.

Theoretical Studies. To get further insight into the effect of molecular structure and electron distribution on the spectroscopic properties of the triphenylamine−benzimidazoles, their geometries and energies were optimized by density functional theory (DFT) calculations at the B3LYP/6-31G** level. The optimized ground-state geometries together with the relevant molecular orbital plots of the HOMOs and LUMOs for the investigated compounds are shown in Figure 4. In general, and in agreement with previous studies,[26] it is seen that the three benzene rings in the tryphenylamine core are nonplanar (with the phenyl rings of the triphenylamine chromophore displaying dihedral angles in the 143.9−147.0° and (−33.4°)−(−36.7°) range with respect to the plane formed by the phenyl ring connected to the benzimidazole moiety) and that the benzimidazole moiety present a slightly distorted conformation with the phenyl linkage of the triphenylamine moiety displaying a dihedral angle in the 7.1−8.9° range with respect to the plane formed by the phenyl group for the compounds investigated (see Figure 4).

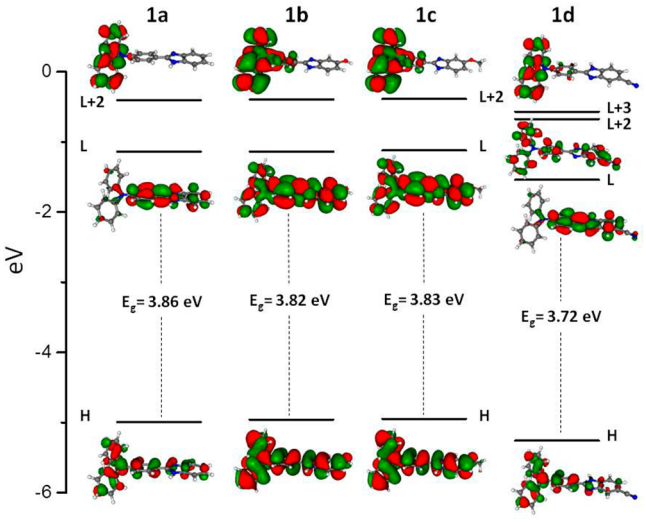

Figure 4. Ground state optimized geometry at the B3LYP/6-31G** level together with the electron distribution of the HOMOs and LUMOs for the relevant molecular orbital energy levels of the triphenylamine−benzimidazole derivatives.

The vertical excitation energies and oscillator strengths are presented in Table 2, and in general, the predicted values show excellent agreement with the values experimentally obtained. In addition, from the oscillator strength values presented in Table 2 it can be seen that these accurately reproduce the relative intensity of the room temperature absorption bands (see Table 2 and Figure 1), thus giving further support for the optimized ground-state geometries. The TD-DFT excited-state calculations also helped us to assign the experimental bands. For all the samples investigated the observed lowest energy absorption bands (and strongest bands) are associated to the predicted $S_0 \rightarrow S_1$ transitions (HOMO→LUMO); see Figure 4. The lower intensity absorption band located at higher energy for compounds **1a** and **1d** (centered at 295 nm) is associated with the $S_0 \rightarrow S_3$ transition, although for **1a** this transition involves the HOMO→LUMO+2 orbitals while for **1d** the predicted transition display contributions from both the HOMO→LUMO+2 and from the HOMO→LUMO+3 (major contribution); see Figure 4. For the triphenylamine-benzimidazoles **1b** and **1c**, functionalized with the electron donor substituents, the bands centered at 300 nm are attributed to the $S_0 \rightarrow S_4$ transition which involves the HOMO→LUMO +2 orbitals.

From the molecular orbital contours (Figure 4) it is possible to see that for compounds **1a** and **1d** the density of the HOMO orbital is mainly located in the triphenylamine moiety while for **1b** and **1c** the electron density is spread over the entire molecule. The electron density of the LUMO shows, in general, a decrease in the electron density on the triphenylamine moiety (donor) and a concomitant increase in the electron-acceptor benzimidazole unit. This behavior is in agreement with previous theoretical studies on similar electron donor−acceptor molecules where the lowest energy absorption band was associated with a charge transfer (CT) type $\pi-\pi^*$ transition from the HOMO to the LUMO orbitals.[20,26,38] In addition, the observed higher energy absorption bands (which correspond to the transitions from the HOMO to LUMO+2 or LUMO+3, see Figure 4 and discussion above) were attributed to the locally excited (LE) $\pi-\pi^*$ transition at the triphenylamine moiety.[38] To further investigate the CT character of the lowest energy transition in more detail the absorption and emission spectra of these compounds were also obtained in the nonpolar solvent methylcyclohexane (see Table 2). Comparison between the spectroscopic features in ethanol and methylcyclohexane,

dx.doi.org/10.1021/jo401803u | J. Org. Chem. 2013, 78, 11389−11395

reveals a solvent independent absorption spectra while the fluorescence emission spectra displays a clear solvent dependence with a significant bathochromic shift in the emission wavelength maxima with increasing solvent polarity. The higher solvatochromic shifts seen in the fluorescence emission spectra compared to those in the absorption spectra suggest an excited state with stronger CT character thus supporting the behavior found in the electron density distribution of the LUMO for the investigated compounds.[39,40]

CONCLUSIONS

Four new triphenylamine−benzimidazole derivatives functionalized at position 5 of the benzimidazole moiety have been synthesized in good to excellent yields from commercially available reagents, using a simple methodology of synthesis and purification. The compounds showed high fluorescence quantum yields, which makes them suitable candidates for light-emitting applications. From the overall data, it was shown that the radiative decay is dominant with negligible efficiency of the singlet−triplet intersystem crossing channel. It was also found that substitution of the triphenylamine−benzimidazole moiety with electron-donating or -withdrawing groups changes its spectral properties; however, the photophysical properties were found to not change significantly. Theory shows that the predicted HOMO−LUMO gaps are in very good agreement with the experimentally estimated optical band gaps and the presence of a CT transition involving the triphenylamine (donor) and the electron-acceptor benzimidazole units, with particular emphasis in compound **1d**.

EXPERIMENTAL SECTION

General Procedure for the Synthesis of Benzimidazoles 1a−d. A solution of the appropriate *o*-nitroaniline (1 equiv) and 4-(*N*,*N*-diphenylamino)benzaldehyde (1 equiv) in DMSO (3 mL) was treated with $Na_2S_2O_4$ (3 equiv), dissolved in a small volume of water, and heated at reflux with stirring for 4 h. The mixture was then cooled to room temperature and the product precipitated during neutralization with NH_4OH 5 M. The precipitate was filtered, washed with diethyl ether, and dried to give the product which was recrystallized from chloroform.

*2-(4′-(N,N-Diphenylamino)phenyl)-1,3-benzimidazole (**1a**):* yellow solid (61 mg, 89%); mp 227.1−227.9 °C; ^{1}H NMR (400 MHz, DMSO-d_6) δ = 7.04 (d, 2H, J = 8.8 Hz), 7.16−7.22 (m, 6H), 7.38−7.43 (m, 6H), 7.67−7.70 (m, 2H), 8.03 (d, 2H, J = 8.8 Hz); ^{13}C NMR (100.6 MHz, DMSO-d_6) δ = 114.0, 117.0, 119.9, 124.2, 125.0, 125.8, 128.7, 130.0, 134.5, 145.8, 149.7, 150.7; IR (Nujol) ν = 3401, 3060, 1866, 1806, 1631, 1613, 1590, 1503, 1335, 1278, 1205, 1080, 894, 841, 752, 699 cm^{-1}; MS (EI) m/z 361 (M$^+$, 100), 360 (10); HRMS (EI) m/z for $C_{25}H_{19}N_3$ calcd 361.1579, found 361.1583.

*5-Hydroxy-2-(4′-(N,N-diphenylamino)phenyl)-1,3-benzimidazole (**1b**):* yellow solid (59 mg, 87%); mp 252.8−253.3 °C; ^{1}H NMR (400 MHz, DMSO-d_6) δ = 6.84 (dd, 1H, J = 8.8 and 2.0 Hz), 6.96 (d, 1H, J = 2.0 Hz), 7.02 (d, 2H, J = 8.8 Hz), 7.14−7.20 (m, 6H), 7.37−7.41 (m, 4H), 7.47 (d, 1H, J = 8.8 Hz), 7.96 (d, 2H, J = 8.8 Hz), 9.66 (s, 1H); ^{13}C NMR (100.6 MHz, DMSO-d_6) δ = 98.2, 113.8, 115.0, 117.9, 120.3, 124.8, 125.6, 128.2, 130.0, 135.3, 146.0, 148.7, 150.2, 155.0; IR (Nujol) ν = 3410, 1634, 1611, 1590, 1335, 1297, 1267, 1203, 1169, 1127, 1073, 958, 830, 759, 722, 697 cm^{-1}; MS (EI) m/z 377 (M$^+$, 69), 213 (23), 191 (33), 151 (31), 137 (32), 123 (36), 111 (56), 98 (100), 83 (96), 69 (84); HRMS (EI) m/z for $C_{25}H_{19}N_3O$ calcd 377.1528, found 377.1515.

*5-Methoxy-2-(4′-(N,N-diphenylamino)phenyl)-1,3-benzimidazole (**1c**):* yellow solid (65 mg, 91%); mp 244.7−245.4 °C; ^{1}H NMR (400 MHz, DMSO-d_6) δ = 3.83 (s, 3H), 6.99−7.04 (m, 3H), 7.13 (d, 1H, J = 2.0 Hz), 7.13−7.21 (m, 6H), 7.38−7.42 (m, 4H), 7.57 (d, 1H, J = 8.8 Hz), 7.99 (d, 2H, J = 8.8 Hz); ^{13}C NMR (100.6 MHz, DMSO-d_6) δ = 55.7, 96.6, 113.7, 114.9, 117.4, 120.1, 124.9, 125.7, 128.4, 130.0, 135.2, 145.9, 149.2, 150.4, 157.1; IR (Nujol) ν = 3354, 1637, 1611, 1588, 1336, 1270, 1202, 1160, 1023, 968, 838, 753, 735, 695 cm^{-1}; MS (EI) m/z 391 (M$^+$, 100), 376 (55), 348 (7), 185 (10), 129 (13), 97 (21), 83 (19); HRMS (EI) m/z for $C_{26}H_{21}N_3O$ calcd 391.1685, found 391.1689.

*5-Cyano-2-(4′-(N,N-diphenylamino)phenyl)-1,3-benzimidazole (**1d**):* yellow solid (67 mg, 95%); mp 275.6−276.7 °C; ^{1}H NMR (400 MHz, DMSO-d_6) δ = 7.02 (dd, 2H, J = 8.8 and 2.0 Hz), 7.15−7.22 (m, 6H), 7.38−7.42 (m, 4H), 7.69 (dd, 1H, J = 8.4 and 1.6 Hz), 7.78 (d, 1H, J = 8.8 Hz), 8.06 (dd, 2H, J = 8.8 and 2.0 Hz), 8.16 (d, 1H, J = 2.0 Hz); ^{13}C NMR (100.6 MHz, DMSO-d_6) δ = 105.1, 115.2, 118.1, 119.3, 119.5, 119.9, 124.9, 125.8, 126.9, 128.8, 130.0, 136.6, 139.1, 145.9, 150.6, 153.3; IR (Nujol) ν = 3352, 2229, 1609, 1587, 1344, 1294, 1202, 1063, 831, 758, 739, 698 cm^{-1}; MS (EI) m/z 386 (M$^+$, 100), 385 (M$^+$, 11); HRMS (EI) m/z for $C_{26}H_{18}N_4$ calcd 386.1531, found 386.1538.

Materials and Instrumentation. Melting points were measured on a melting point apparatus. Thin-layer chromatography (TLC) was carried out on 0.25 mm thick precoated silica plates, and spots were visualized under UV light. IR spectra were determined on a spectrophotometer. NMR spectra were obtained with an operating frequency of 400 MHz for ^{1}H and 100.6 MHz for ^{13}C using the solvent peak as internal reference at 25 °C. All chemical shifts are given in ppm using δ_H Me_4Si = 0 ppm as reference, and J values are given in Hz. Assignments were made by comparison of chemical shifts, peak multiplicities, and J values and were supported by spin decoupling-double resonance and bidimensional heteronuclear correlation techniques. Mass spectrometry analyses were performed using electron-impact ionization technique. Thermogravimetric analysis of samples was carried out using a TGA instrument, under high purity nitrogen supplied at a constant 50 mL min^{-1} flow rate. All samples were subjected to a 20 °C min^{-1} heating rate and were characterized between 25 and 800 °C. All reagents were used as received.

Absorption and fluorescence spectra were recorded on a UV−vis spectrometer and on a spectrofluorimeter with 450 W as excitation source and double grating monochromators, respectively.

The molar extinction coefficients (ε) were obtained from absorption spectral measurements using six solutions of different concentrations and the slope of plots of the absorption vs concentration.

The fluorescence quantum yields were measured using quinine sulfate (ϕ_F = 0.545) in 0.5 M H_2SO_4 solution as standard. Fluorescence decays were measured using home-built nanosecond[41] and picosecond[42] time correlated single photon counting (TCSPC) apparatus described elsewhere. The fluorescence decays and the instrumental response function (IRF) were collected using a time scale of 1024 channels, until 5 × 10^3 counts at maximum were reached. Deconvolution of the fluorescence decay curves was performed using the modulating function method as implemented by G. Striker in the SAND program as previously reported.[43]

The ground-state molecular geometry was optimized using the density functional theory (DFT) by means of the Gaussian 03 program[44] at the B3LYP/6-31G** level.[45,46] Optimal geometries were determined on isolated entities in a vacuum, and no conformation restrictions were imposed. For the resulting optimized geometries time dependent DFT calculations (using the same functional and basis set as those in the previously calculations) were performed to predict the vertical electronic excitation energies. Molecular orbital contours were plotted using Molekel 5.4.

The experimental setup used to obtain triplet spectra and triplet yields has been described elsewhere.[41,47] First-order kinetics was observed for the decay of the lowest triplet state. Special care was taken in determining triplet yields, namely to have optically matched dilute solutions (abs ≈ 0.2 in a 10 mm square cell) and low laser energy (≤2 mJ) to avoid multiphoton and T−T annihilation effects.

The triplet molar absorption coefficients (ε_T) were obtained by the singlet depletion technique applying the well-known relationship (eq 1)[48]

$$\varepsilon_T = \frac{\varepsilon_S \times \Delta OD_T}{\Delta OD_S} \quad (1)$$

where both ΔOD_S and ΔOD_T are obtained from the triplet−singlet difference transient absorption spectra and ε_S correspond to the ground state molar extinction coefficients.

The ϕ_T values were obtained by comparing the triplet ΔO.D. at 525 nm of a benzene solution of benzophenone (@ λ_{exc} = 355 nm) with that of the compounds (optically matched at the laser wavelength) as described elsewhere.[41,47]

Room-temperature singlet oxygen phosphorescence was detected at 1270 nm using a Hamamatsu R5509-42 photomultiplier, cooled to 193 K in a liquid nitrogen chamber, following laser excitation of aerated solutions at 355 nm, with an adapted Applied Photophysics flash kinetic spectrometer, as reported elsewhere.[49] 1*H*-Phenalen-1-one (perinaphthenone) in toluene (λ_{exc} = 355 nm), ϕ_Δ = 0.93, was used as the standard.[50]

■ ASSOCIATED CONTENT

Supporting Information

Room-temperature absorption and fluorescence spectra for the triphenylamine−benzimidazole derivatives in methylcyclohexane solution, Cartesian coordinates, and absolute energy values for the optimized geometries together ^{1}H and ^{13}C NMR spectra of compounds **1a−d**. This material is available free of charge via the Internet at http://pubs.acs.org.

■ AUTHOR INFORMATION

Corresponding Authors

*E-mail: sseixas@ci.uc.pt.

*E-mail: mfox@quimica.uminho.pt.

Notes

The authors declare no competing financial interest.

■ ACKNOWLEDGMENTS

Thanks are due to Fundação para a Ciência e Tecnologia (Portugal) and FEDER-COMPETE for financial support through Centro de Química-UM [PEst-C/QUI/UI0686/2011 (F-COMP-01-0124-FEDER-022716)], Centro de Química-UC (PEst-C/QUI/UI0313/2011), and Program C2008-DRH05-11-842. A postdoctoral grant to R.M.F.B. (SFRH/BPD/79333/2011) is also acknowledged. The NMR spectrometer Bruker Avance III 400 is part of the National NMR Network and was purchased with funds from FCT and FEDER.

■ REFERENCES

(1) Pina, J.; Burrows, H. D.; Seixas de Melo, J. S. Excited state dynamics in π-conjugated polymers. In *Specialist Periodic Reports in Photochemistry*; Albini, A., Ed.; Royal Society of Chemistry: Cambridge, UK, 2011; Vol. *39*, pp 30−64.

(2) Zade, S. S.; Zamoshchik, N.; Bendikov, M. *Acc. Chem. Res.* **2011**, *44* (1), 14−24.

(3) Friend, R. H.; Gymer, R. W.; Holmes, A. B.; Burroughes, J. H.; Marks, R. N.; Taliani, C.; Bradley, D. D. C.; Dos Santos, D. A.; Bredas, J. L.; Logdlund, M.; Salaneck, W. R. *Nature* **1999**, *397* (6715), 121−128.

(4) Falzon, M. F.; Wienk, M. M.; Janssen, R. A. J. *J. Phys. Chem. C* **2011**, *115* (7), 3178−3187.

(5) Liu, L.; Patra, A.; Scherf, U.; Kissel, T. *Macromol. Biosci.* **2012**, *12* (10), 1384−1390.

(6) Zhong, C. M.; Duan, C. H.; Huang, F.; Wu, H. B.; Cao, Y. *Chem. Mater.* **2011**, *23* (3), 326−340.

(7) Tao, Y. T.; Yang, C. L.; Qin, J. G. *Chem. Soc. Rev.* **2011**, *40* (5), 2943−2970.

(8) Sasabe, H.; Kido, J. *Chem. Mater.* **2011**, *23* (3), 621−630.

(9) Tang, C.; Liu, X. D.; Liu, F.; Wang, X. L.; Xu, H.; Huang, W. *Macromol. Chem. Phys.* **2013**, *214* (3), 314−342.

(10) Lu, J.; Xia, P. F.; Lo, P. K.; Tao, Y.; Wong, M. S. *Chem. Mater.* **2006**, *18* (26), 6194−6203.

(11) Sonntag, M.; Kreger, K.; Hanft, D.; Strohriegl, P.; Setayesh, S.; de Leeuw, D. *Chem. Mater.* **2005**, *17* (11), 3031−3039.

(12) Liao, Y.-L.; Lin, C.-Y.; Wong, K.-T.; Hou, T.-H.; Hung, W.-Y. *Org. Lett.* **2007**, *9* (22), 4511−4514.

(13) Molina, P.; Tarraga, A.; Oton, F. *Org. Biomol. Chem.* **2012**, *10* (9), 1711−1724.

(14) Formica, M.; Fusi, V.; Giorgi, L.; Micheloni, M. *Coord. Chem. Rev.* **2012**, *256* (1−2), 170−192.

(15) Lai, M.-Y.; Chen, C.-H.; Huang, W.-S.; Lin, J. T.; Ke, T.-H.; Chen, L.-Y.; Tsai, M.-H.; Wu, C.-C. *Angew. Chem., Int. Ed.* **2008**, *47* (3), 581−585.

(16) Gong, S.; Zhao, Y.; Wang, M.; Yang, C.; Zhong, C.; Qin, J.; Ma, D. *Chem.—Asian J.* **2010**, *5* (9), 2093−2099.

(17) Sarma, M.; Chatterjee, T.; Ghanta, S.; Das, S. K. *J. Org. Chem.* **2011**, *77* (1), 432−444.

(18) Estrada, L. A.; Neckers, D. C. *J. Org. Chem.* **2009**, *74* (21), 8484−8487.

(19) Ge, Z.; Hayakawa, T.; Ando, S.; Ueda, M.; Akiike, T.; Miyamoto, H.; Kajita, T.; Kakimoto, M.-a. *Adv. Funct. Mater.* **2008**, *18* (4), 584−590.

(20) Jeong, S.; Kim, M.-K.; Kim, S. H.; Hong, J.-I. *Org. Electron.* **2013**, *14* (10), 2497−2504.

(21) Batista, R. M. F.; Ferreira, R. C. M.; Raposo, M. M. M.; Costa, S. P. G. *Tetrahedron* **2012**, *68* (36), 7322−7330.

(22) Esteves, C. I. C.; Raposo, M. M. M.; Costa, S. P. G. *Tetrahedron* **2010**, *66* (38), 7479−7486.

(23) Batista, R. M. F.; Costa, S. P. G.; Raposo, M. M. M. *J. Photochem. Photobiol. A-Chem.* **2013**, *259*, 33−40.

(24) Batista, R. M. F.; Costa, S. P. G.; Belsley, M.; Raposo, M. M. M. *Tetrahedron* **2007**, *63* (39), 9842−9849.

(25) Batista, R. M. F.; Oliveira, E.; Costa, S. P. G.; Lodeiro, C.; Raposo, M. M. M. *Talanta* **2011**, *85* (5), 2470−2478.

(26) Zhou, L.; Jia, C.; Wan, Z.; Li, Z.; Bai, J.; Zhang, L.; Zhang, J.; Yao, X. *Dyes Pigm.* **2012**, *95* (3), 743−750.

(27) Yang, D. L.; Fokas, D.; Li, J. Z.; Yu, L. B.; Baldino, C. M. *Synthesis* **2005**, *1*, 47−56.

(28) Valeur, B., *Molecular Fluorescence: Principles and Applications*; Wiley-VCH: Weinheim, 2002.

(29) Moss, K. C.; Bourdakos, K. N.; Bhalla, V.; Kamtekar, K. T.; Bryce, M. R.; Fox, M. A.; Vaughan, H. L.; Dias, F. B.; Monkman, A. P. *J. Org. Chem.* **2010**, *75* (20), 6771−6781.

(30) Zheng, Y. H.; Batsanov, A. S.; Jankus, V.; Dias, F. B.; Bryce, M. R.; Monkman, A. P. *J. Org. Chem.* **2011**, *76* (20), 8300−8310.

(31) Gonzàlez, S. R.; Orduna, J.; Alicante, R.; Villacampa, B.; McGee, K. A.; Pina, J.; Seixas de Melo, J.; Schwaderer, K. M.; Johnson, J. C.; Blackorbay, B. A. *J. Phys. Chem. B* **2011**, *115* (36), 10573−10585.

(32) Kulkarni, A. P.; Zhu, Y.; Babel, A.; Wu, P.-T.; Jenekhe, S. A. *Chem. Mater.* **2008**, *20* (13), 4212−4223.

(33) Pina, J.; Seixas de Melo, J. S.; Koenen, N.; Scherf, U. *J. Phys. Chem. B* **2013**, *117* (24), 7370−7380.

(34) Di Paolo, R. E.; Seixas de Melo, J.; Pina, J.; Burrows, H. D.; Morgado, J.; Maçanita, A. L. *ChemPhysChem* **2007**, *8* (18), 2657−2664.

(35) Dias, F. B.; Pollock, S.; Hedley, G.; Palsson, L. O.; Monkman, A.; Perepichka, I. I.; Perepichka, I. F.; Tavasli, M.; Bryce, M. R. *J. Phys. Chem. B* **2006**, *110* (39), 19329−19339.

(36) Li, H. Y.; Batsanov, A. S.; Moss, K. C.; Vaughan, H. L.; Dias, F. B.; Kamtekar, K. T.; Bryce, M. R.; Monkman, A. P. *Chem. Commun.* **2010**, *46* (26), 4812−4814.

(37) Jayabharathi, J.; Thanikachalam, V.; Jayamoorthy, K. *Photochem. Photobiol. Sci.* **2013**, *12* (10), 1761−1773.

(38) Ge, Z.; Hayakawa, T.; Ando, S.; Ueda, M.; Akiike, T.; Miyamoto, H.; Kajita, T.; Kakimoto, M.-a. *Chem. Mater.* **2008**, *20* (7), 2532−2537.

(39) Angulo, G.; Dobkowski, J.; Kapturkiewicz, A.; Maciolek, K. *J. Photochem. Photobiol. A-Chem.* **2010**, *213* (2−3), 101−106.
(40) Kulkarni, A. P.; Wu, P.-T.; Kwon, T. W.; Jenekhe, S. A. *J. Phys. Chem. B* **2005**, *109* (42), 19584−19594.
(41) Pina, J.; Burrows, H. D.; Becker, R. S.; Dias, F. B.; Maçanita, A. L.; Seixas de Melo, J. *J. Phys. Chem. B* **2006**, *110*, 6499−6505.
(42) Pina, J.; Seixas de Melo, J.; Burrows, H. D.; Maçanita, A. L.; Galbrecht, F.; Bunnagel, T.; Scherf, U. *Macromolecules* **2009**, *42* (5), 1710−1719.
(43) Striker, G.; Subramaniam, V.; Seidel, C. A. M.; Volkmer, A. *J. Phys. Chem. B* **1999**, *103* (40), 8612−8617.
(44) Frisch, M. J.; Trucks, G. W.; Schlegel, H. B.; Scuseria, G. E.; Robb, M. A.; Cheeseman, J. R.; Montgomery, J. A., Jr.; Vreven, T.; Kudin, K. N.; Burant, J. C.; Millam, J. M.; Iyengar, S. S.; Tomasi, J.; Barone, V.; Mennucci, B.; Cossi, M.; Scalmani, G.; Rega, N.; Petersson, G. A.; Nakatsuji, H.; Hada, M.; Ehara, M.; Toyota, K.; Fukuda, R.; Hasegawa, J.; Ishida, M.; Nakajima, T.; Honda, Y.; Kitao, O.; Nakai, H.; Klene, M.; Li, X.; Knox, J. E.; Hratchian, H. P.; Cross, J. B.; Bakken, V.; Adamo, C.; Jaramillo, J.; Gomperts, R.; Stratmann, R. E.; Yazyev, O.; Austin, A. J.; Cammi, R.; Pomelli, C.; Ochterski, J. W.; Ayala, P. Y.; Morokuma, K.; Voth, G. A.; Salvador, P.; Dannenberg, J. J.; Zakrzewski, V. G.; Dapprich, S.; Daniels, A. D.; Strain, M. C.; Farkas, O.; Malick, D. K.; Rabuck, A. D.; Raghavachari, K.; Foresman, J. B.; Ortiz, J. V.; Cui, Q.; Baboul, A. G.; Clifford, S.; Cioslowski, J.; Stefanov, B. B.; Liu, G.; Liashenko, A.; Piskorz, P.; Komaromi, I.; Martin, R. L.; Fox, D. J.; Keith, T.; Al-Laham, M. A.; Peng, C. Y.; Nanayakkara, A.; Challacombe, M.; Gill, P. M. W.; Johnson, B.; Chen, W.; Wong, M. W.; Gonzalez, C.; Pople, J. A. *Gaussian 03, Revision C.02*; Gaussian, Inc.: Wallingford, CT, 2004.
(45) Becke, A. D. *J. Chem. Phys.* **1993**, *98* (2), 1372−1377.
(46) Francl, M. M.; Pietro, W. J.; Hehre, W. J.; Binkley, J. S.; Gordon, M. S.; Defrees, D. J.; Pople, J. A. *J. Chem. Phys.* **1982**, *77* (7), 3654−3665.
(47) Pina, J.; Seixas de Melo, J.; Burrows, H. D.; Bilge, A.; Farrell, T.; Forster, M.; Scherf, U. *J. Phys. Chem. B* **2006**, *110* (31), 15100−15106.
(48) Ian, C.; Gordon, L. H. *J. Phys. Chem. Ref. Data* **1986**, *15* (1), 1−250.
(49) Pina, J.; Seixas de Melo, J. *Phys. Chem. Chem. Phys.* **2009**, *11* (39), 8706−8713.
(50) Oliveros, E.; Suardimurasecco, P.; Aminiansaghafi, T.; Braun, A. M.; Hansen, H. J. *Helv. Chim. Acta* **1991**, *74* (1), 79−90.